Zeitschrift für Geomorphologie, Vol. 57 (2013), Suppl. 4, 201–228 **Article**
Published online September 2013

Holocene coastal stratigraphy, coastal changes and potential palaeoseismological implications inferred from geo-archives in Central Chile (29–32° S)

Simon Matthias May, Anna Pint, Gilles Rixhon, Dieter Kelletat, Volker Wennrich and Helmut Brückner

With 8 figures and 2 tables

Abstract. Coastal geomorphology and the stratigraphy of coastal geoarchives record past coastal and fluctuations of coastal environments. In addition, these archives potentially store traces of past extreme events such as earthquakes and tsunamis, severe storms, and major floodings of the coastal hinterland, e.g. due to El Niño conditions. Studying their characteristics may thus improve the knowledge of past frequency and magnitude patterns of such extreme events. For instance, large scaled spatial information about past earthquakes is needed for the understanding and estimation of seismo-tectonic processes. Misinterpretations in the size of preceding earthquakes may lead to incorrect strain balance estimations along megathrusts. Thus, fundamental research on the occurrence of past earthquakes is needed, which can be reflected in sudden or long-term coastal changes.

Using sedimentological, geomorphological and microfaunal evidence, coeval geomorphodynamic and palaeoenvironmental changes at four different locations between 29° 50' and 32° 20' S in Central Chile were identified in estuary systems, coastal swamps and coastal plains. The results may represent possible indirect evidence for palaeoseismicity, affecting the coastal system by vertical tectonic movements. Changes of coastline elevation, morphodynamic activity and/or coastal environments, as well as the formation of a liquefaction layer took place during the last c. 400 years. Moreover, major flooding events related to strong El Niño conditions are assumed to have influenced the coastal stratigraphy by depositing high energy fluvial deposits. Our results suggest that the coastal environment, geomorphology and stratigraphy are considerably influenced by tectonic processes in the study area; a relation of the presented findings to the 1730 Great Valparaíso Earthquake is assumed. In general, the findings may encourage the implementation of comparable detailed studies, which may ultimately contribute to a better understanding of the Holocene coastal evolution and its relation to palaeoseismicity in Central Chile.

Key words: Central Chile, coastal change, palaeoseismology, El Niño, liquefaction, tectonic subsidence/uplift

Zusammenfassung. Küstennahe Geoarchive wie Ästuarsysteme und Küstensümpfe haben das Potential, Informationen über holozäne Küstenentwicklungen und paläoökologische Veränderungen zu speichern. Mit ihrer Hilfe können darüber hinaus wertvolle Rückschlüsse auf Frequenz und Magnitude vergangener Extremereignisse wie Erdbeben, Tsunamis, Sturmfluten oder El Niño induzierte Überflutungen gezogen werden. Beispielsweise sind Erkenntnisse über die räumlichen Ausmaße vergangener Erdbeben für das Verständnis seismo-tektonischer Prozesse von großer Bedeutung. Fehlinterpretationen bezüglich der Größe von Paläobeben können zur fehlerhaften Abschätzung von Krustendeformationsraten oder Spannungsbilanzen entlang von Subduktionszonen und damit der unmittelbaren Erdbebengefahr führen. Nach wie vor werden aus diesem Grunde neue Erkenntnisse zum Auftreten vergangener Erdbeben benötigt, die sich in plötzlichen oder langfristigen Küstenveränderungen widerspiegeln können.

Basierend auf sedimentologischen, geomorphologischen und mikrofaunistischen Untersuchungen in küstennahen Geoarchiven wurden geomorphodynamische und paläoökologische Veränderungen in vier unterschiedlichen zentralchilenischen Küstengebieten zwischen 29° 50' und 32° 20' S identifiziert. Die hier

www.borntraeger-cramer.de
DOI: 10.1127/0372-8854/2013/S-00154
0372-8854/13/S-00154 $ 6.75

vorgestellten Ergebnisse zeigen indirekte Belege für paläoseimische Ereignisse, die zu vertikalen Krustenbewegungen in der untersuchten Küstenregion geführt haben. Sowohl Verlagerungen des Küstenverlaufs, Veränderungen der morphodynamischen Aktivität und/oder der küstennahen ökologischen Bedingungen als auch die Entstehung einer möglichen Liquefaktionslage wurde auf eine Zeit innerhalb der letzten 400 Jahre datiert. Ein Zusammenhang mit dem großen Valparaíso Erdbeben im Jahre 1730 wird vermutet. Des Weiteren beeinflussten größere El Niño Ereignisse die Stratigraphie der küstennahen Sedimentsequenzen in Form von hochenergetischen fluvialen Ablagerungen in jüngerer Zeit. Unsere Ergebnisse deuten darauf hin, dass die ökologischen Bedingungen küstennaher Geoarchive sowie die küstennahe Geomorphologie und Stratigraphie im Arbeitsgebiet von tektonischen Prozessen gesteuert werden. Unsere Ergebnisse unterstreichen den Nutzen ähnlicher, detaillierter Studien, die letztlich zu einem besseren Verständnis der holozänen Küstenentwicklung und ihrer Beziehung zur paläoseismischen Vergangenheit in Zentralchile beitragen können.

1 *Introduction*

Coastal geomorphology and the stratigraphical succession of coastal geoarchives record past coastal changes and fluctuations of coastal environments. In addition, these archives have the potential to store traces of past extreme events such as earthquakes and tsunamis, severe storms, and major floodings of the coastal hinterland, the latter occurring e.g. during strong El Niño conditions. By studying their sedimentological and ecological characteristics and their chronology, coastal changes throughout time can be reconstructed. Their use as recorders of past events may enlarge the temporal frame of historical event records, improving the information on past frequency and magnitude of such extreme events.

In the context of seismic events, the recent exceptional earthquakes and the following devastating tsunamis – in Southeast Asia (December 26th, 2004, Sumatra–Andaman Earthquake), in Chile (February 27th, 2010, Maule Earthquake), and in Japan (March 11th, 2011, Tohoku-oki Earthquake) – have demonstrated the high vulnerability of coastlines adjacent to plate boundaries. These outstanding events generated new seismological information since they were the first to be studied by dense networks of geodetic observations (Hanson 2005, Heki 2011). However, the recent observations also revealed knowledge gaps in earthquake sciences (Geller 2011). Misinterpretations of the size of preceding historical earthquakes may lead to an overestimation of strain release in megathrust segments and incorrect strain balance estimations. Resulting discrepancies in the calculation of strain accumulation and slip deficits underline the imperative of fundamental research on the occurrence of past earthquakes and tsunamis (e.g. Stein 2008). According to Yeats et al. (1997), earthquake magnitudes may generally be related to the length of the associated rupture zone. In Chile, the 2010 Maule event was related to a ~500 km rupture of the megathrust segment off Concepción and Constitución (Moreno et al. 2010, Lorito et al. 2011), while the 1960 Valdivia megaquake ruptured a megathrust segment of more than 1000 km length directly to the south (Plafker & Savage 1970, Cifuentes 1989, Moreno et al. 2009) (Figs. 1 and 2).

Although the theory of seismic gaps and their potential for the prediction of earthquakes has been questioned during the last decades (Kagan & Jackson 1991, Stein 2008, Geller 2011), the 2010 Maule Earthquake (M_w 8.8) in South Central Chile occurred in a since 1835 inactive megathrust segment (Campos et al. 2002, Moreno et al. 2010, 2011, Heki 2011), i.e. a seismic gap, where elastic strain has accumulated long enough to produce a large earthquake (see also Dewey & Spence 1979). In this regard, the differentiation of past great (M_w 8–9) and giant earthquakes

($M_w > 9$) (Heaton & Hartzell 1987) is of particular importance, the latter having longer recurrence rates (up to 500 years or similar scale) and releasing much larger energy (Satake & Atwater 2007), depending on the characteristics of the rupture zone. In many earthquake-prone areas, in particular in the Americas, low population density hindered the compilation of reliable and continuous reports earlier than the middle of the 19th century. Historical accounts (e.g., Berninghausen 1962, Lockridge 1985, Lomnitz 2004) thus possibly do not report on the occurrence of giant earthquakes, although they may be part of the seismic cycle in the regarded area (Stein 2006). Additionally, over- and/or understatements of earthquake effects must be considered, and strong earthquakes may still be hidden in historical archives (Lomnitz 2004, Cisternas et al. 2012). Thus, giant earthquakes may also occur where no comparable events were previously reported or have not been expected to date (Geller 2011, Ozawa et al. 2011). However, for the understanding and estimation of seismo-tectonic processes, large scaled spatial information about past giant earthquakes is needed since these events particularly contribute to strain release along megathrusts.

In the case of shallow thrust earthquakes, rupture lengths and the spatial distribution of their tsunami deposits or other palaeoseismological indications are closely related (Lorito et al. 2011). Several studies have underlined the importance of studies on coastal geo-archives during the last decades such as combined palaeoseismological and palaeotsunami research and detailed investigations on historical reports (Clague et al. 2000, Sawai 2001, Cisternas et al. 2005, Kelsey et al. 2005, Jankaew et al. 2008, Fujino et al. 2009, Brill et al. 2011), although the variability of event deposits and the incompleteness of geological records may complicate a palaeoseismological interpretation. Evidence for past seismic events may also be brought by the detection of liquefaction structures in suitable geological archives (Kelsey et al. 2002, Guarnieri et al. 2009, Martin & Bourgeois 2012). Likewise, successions of brackish estuarine sediments and freshwater peat, reflected by microfaunal assemblages, potentially reveal changes in the local relative sea level, related to uplift or subsidence of coastal areas during seismic events; they can be used for palaeoseismological interpretations (Atwater 1987, Atwater et al. 2004a, b, Sawai 2001, Sawai et al. 2004, Reinhardt et al. 2010).

In northern Central Chile, the 1730 Great Valparaíso Earthquake is regarded as the most prominent historical event, though little is known about its impacts for large parts of the coastline (Nishenko 1985, Lomnitz 2004). For several further earthquakes, e.g. the 1647 Great Santiago Earthquake, co- and postseismic tectonic movements are known as well (Arana 2009). In this area, sudden or long-term coastal change due to vertical tectonic movements is expected at least on a local scale, involving environmental changes as well as fluvial response (e.g., incision) in river mouth areas, which may be detected by palaeoenvironmental, sedimentological and geomorphological criteria (e.g., Wells & Goff 2006, May et al. 2012). Against this background, this paper uses sedimentary archives from four coastal areas along the Central Chilean segment between 29° 50' S and 32° 20' S to detect traces of late Holocene coastal changes and extreme events by means of geomorphological, sedimentological and microfaunal investigations (Fig. 1). Where possible, a correlation to tectonic events will be discussed, providing (i) indirect implications for late Holocene and/or historical palaeoseismicity in Central Chile, and (ii) a basis for further detailed studies.

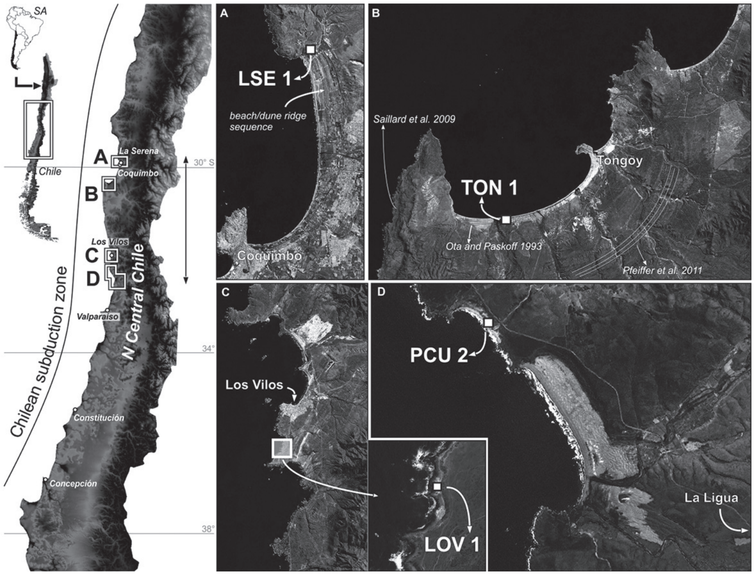

Fig. 1. Overview and general setting of northern Central Chile. (A) Coquimbo Bay; core LSE 1 was carried out in the very northern part of the bay, at the estuary river mouth of the Quebrada Teatinos. (B) Bay of Tongoy; coring site TON 1 is located in the coastal swamp in the river mouth of the Quebrada Pachingo. (C) Sampling site LOV 6, south of Los Vilos. The coastal section is characterised by pocket-like beaches and ~10 m high cliffs. (D) Pichicuy Bay with the location of profile PCU 2 where a possible liquefaction unit was detected (map based on SRTM data; images of study sites from Google Earth).

2 *Study area*

2.1 *Tectonic setting*

2.1.1 *General tectonic setting*

Chile belongs to the most earthquake-prone areas worldwide as it experiences one great earthquake of $M_w > 8$ every five to ten years (Barrientos 2007, Vigny et al. 2009). In each segment of the Chile subduction zone (Beck et al. 1998), these events return every 80–130 years (see Fig. 2, Barrientos et al. 2004). Earthquakes occur along the Andean (also South American) subduction zone or megathrust, where the oceanic Nazca Plate subducts below the South American Plate (cf. Barrientos et al. 2004, Moreno et al. 2008). Along this zone, changes of the subduction character and the rupture behavior of related earthquakes are observed both on temporal and spatial scales, explained by the complexity of the subducting Nazca plate comprising seamounts, ridges, fracture zones and trench sediments of varying thickness (Bilek 2010). However, three general seismogenic zones can be recognized in Chile (Barrientos et al. 2004): (i) a zone of shallow (50–0 km), large thrust events occurring along the coast (here, most tsunamigenic earthquakes are generated between 18° S and 46° S); (ii) a zone of large earthquakes of intermediate depth (100–70 km) in the subducting Nazca Plate, both compressional and tensional; and (iii) a zone of very shallow

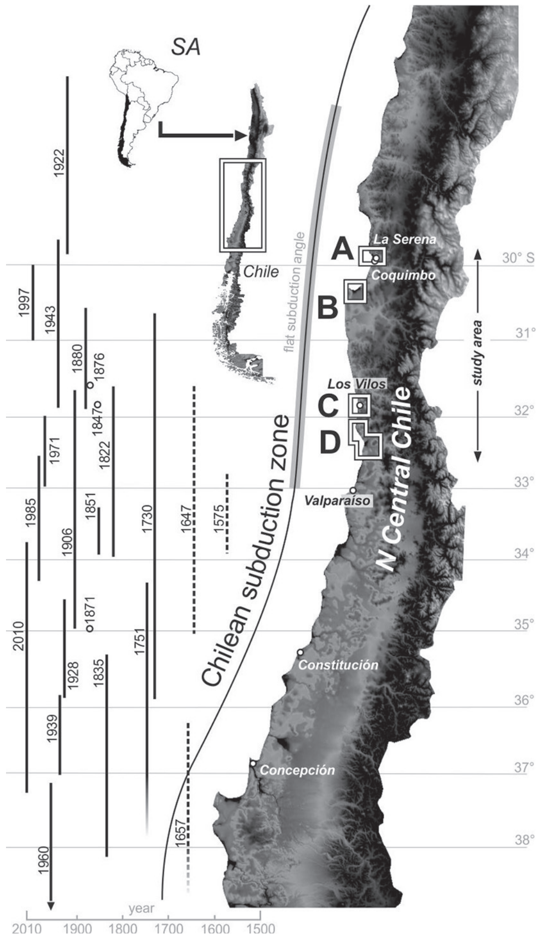

Fig. 2. Rupture lengths and extent of main historical earthquakes between c. 28° S and 38° S, Central Chile (map based on SRTM data; rupture areas based on Kelleher 1972, Nishenko 1985, Comte et al. 1986, Lemoine et al. 2001, Campos et al. 2002, Pardo et al. 2002a, b, Gardi et al. 2006, Vigny et al. 2009, Moreno et al. 2010, Lorito et al. 2011).

seismicity (20–0 km) which notably takes place under the Cordillera of Central Chile. In this latter region (between 28° S and 33° S, Fig. 2), the Nazca Plate is indeed subducted as a flat slab; its dipping angle is below 10° and extends eastward almost horizontally for hundreds of kilometers at intermediate depths (Cahill & Isacks 1992, Pardo et al. 2002a). Seismic coupling is assumed for the area (Gardi et al. 2006, Métois et al. 2012), which is part of the Coquimbo seismic gap (29.5° S –32° S) gap as well (Vigny et al. 2009). Along the Central Chilean coastline, the difference in the angle of the subduction and/or the submarine Juan Fernandez ridge (32° S –33° S) (Nishenko 1985, Fuenzalida et al. 1992, Ranero et al. 2006) are supposed to limit the rupture length and thus the size of possible earthquakes.

2.1.2 *Pleistocene coastal uplift and marine terraces*

Strong earthquakes in Chile are generally associated with vertical crustal movements, such as coastal uplift and/or subsidence (e.g., Plafker & Savage 1970, Nelson & Manly 1992, Melnick et al. 2006, 2012, Vargas et al. 2011). On longer time scales, the high seismicity and tectonic activity is reflected by elevated marine terraces or beach ridge sequences, which are gradually or suddenly isolated from the foreshore dynamics resulting in a prograding pattern of beach ridge systems (e.g., Otvos 2000). Dating these features is crucial to gain insights into displacement rates of crustal segments (e.g., Paskoff 1970, Radtke 1987, Bookhagen et al. 2006, Pfeifer et al. 2011), though other forming processes such as the influence of increased sediment pulses by El Niño events (e.g. Sandweiss 1986) have to be taken into account.

Within the southern part of the study area, little information about structural tectonic elements, local tectonics and Pleistocene marine terraces is available. Recently, cosmogenic nuclide ages (^{10}Be and ^{26}Al) performed on different landforms located at 31.5° S (pediment, marine and fluvial terraces) highlighted (i) a period of relative tectonic stability during the 800–500 ka time span, and (ii) a renewal of coastal uplift later than 500 ka (uplift rate of ~0,3 m/ka, Rodríguez et al. 2013). To the north, ^{10}Be surface exposure ages of wave-cut platforms in the Altos de Talinay, a northwards stretching part of the Coastal Cordillera, revealed long-term averaged uplift rates varying between ~0.1 m/ka and ~1.2 m/ka for the last 700 ka (Saillard et al. 2009, 2012). The five abrasion platforms were correlated with Quaternary sea-level highstands (MIS 1, 5 e, 7 c or e, 9 c and 17). Pleistocene marine terraces and beach ridges characterise the northern part of the so-called Tongoy Palaeobay Depression (TPD, Le Roux et al. 2005, Saillard et al. 2009, 2012), facing the Bay of Tongoy (Pfeiffer et al. 2011). The Puerto Aldea Fault, a steeply eastward dipping normal fault, represents the contact zone between the TPD and the Altos de Talinay and is indicated by a NNW-SSE orientation. According to U-Th dating of molluscs from the TPD palaeo-beach ridges (Saillard et al. 2012), the fault has been inactive at least since the middle Pleistocene (230–320 ka), resulting in a simultaneous uplift history of the two segments since then.

The 15 km long embayment of Coquimbo Bay and the southward lying smaller La Herradura Bay are bordered by sequences of Pleistocene marine terraces, cut into the Neogene Coquimbo formation (e.g., Herm & Paskoff 1967, Paskoff 1970, Radtke 1987, 1989, Leonard & Wehmiller 1992). Average uplift rates in this area are calculated to have been very low during the Pleistocene (1.15-0.2 m/ka; Leonard & Wehmiller 1992).

Northwards of the Coquimbo region (Copiapo area, ~27° S), ^{21}Ne surface exposure ages on marine terraces provided an average uplift rate of ~0.3 m/ka (Quezada et al. 2007). In South Central Chile (Isla Santa Maria, 37° S), a very high uplift trend of about 2 m/ka was detected for the late Quaternary (Melnick et al. 2006), partly due to coseismic uplift during megathrust earthquakes such as the 1835 Concepción earthquake.

2.2 *Palaeoseismicity in Central Chile*

Within the area of Coquimbo (Central Chile, 29.5° S to 32° S), the most recent and well-studied major earthquake (M_w 7.3) struck the Ovalle-Punitaqui area in October 1997 (Lemoine et al. 2001, Pardo et al. 2002b, Gardi et al. 2006). The main shock occurred at intermediate depth (68 km) within the subducted Nazca Plate and had a subvertical rupture plane with an along-slab (down-dip) compressional mechanism; as such, it was a very rare event in Central Chile (Lemoine et al. 2001, Gardi et al. 2006). Since the resumption of earthquake activity in mid-1997, the segment between 29.5° S and 32° S has been the site of a seismic swarm decade, with 12 earthquakes of $M_w > 6$ during this time span (Vigny et al. 2009).

Before that time, three large events have been recorded in this area during early instrumental and historical periods: in 1943, 1880 and 1730. According to Beck et al. (1998), the rupture distance of the 1943 Illapel-earthquake (M_w ~7.9), centered around 31° S, stretched over 100 km (Fig. 2). The two previous events of 1880 and 1730 are suggested to have ruptured this segment as well, but the 1730 Great Valparaíso Earthquake (M_w ~8.5–9.0) extended over a longer segment of the megathrust. According to the distribution of related effects, and damages in the cities of La Serena and Coquimbo (Lomnitz 2004), its rupture probably affected at least a 550 km-long segment, stretching from 30.5° S to 36° S (Comte et al. 1986).

Southward of the Coquimbo segment, further major historical earthquakes struck the region of Valparaíso (33° S) in 1906, 1822 and 1647. While the location of the 1647 Great Santiago Earthquake (M_w ~8.0) epicenter remains ambiguous, coastal uplift is reported in historical documents (Arana 2009), and its ~365 km-long rupture zone was probably similar to the one engendered by the 1906 Valparaíso Earthquake (M_w ~8.6); the latter rupture stretched northwards into the southern part of the study area (Comte et al. 1986). Though probably of smaller rupture, the 1822 event (Fig. 2; M_w ~8.0-8.5) with a likely epicenter close to La Ligua also extended northwards up to Illapel (Fig. 2) and generated a ~3,5 m-high tsunami (Comte et al. 1986, Lomnitz 2004). The 1730 Great Valparaíso Earthquake corresponds to the largest seismic event reported for the last five centuries in whole Central Chile. However, as pointed out by Nishenko (1985), little is known regarding the length of its rupture zone or the intensity of vertical displacements.

In contrast to the 1997 earthquake (see aforementioned references), information on historic – and all the more prehistoric – events and seismic parameters is limited. In South Central Chile, Cisternas et al. (2005) gave valuable insights into the seismic cycle and fault behavior by examining a 2000 year stratigraphical record from the center of the 1960 fault zone (Río Maullín Estuary) based on the detection of palaeotsunami sediments. In contrast to previous calculations, they showed that much of the energy released during the 1960 event resulted from seismic locking since the 1575 Valdivia earthquake (M_w 8–8.5).

For northern Central Chile and notably for the segment between ~30° S and ~32° S, a lack of analogous studies about palaeoseismicity is evident. Consequently, underestimation of earthquake and related tsunami risk, similar to Sumatra or northeastern Japan in the recent past, may be true for northern Central Chile at present. Indeed, based on the available historical accounts and due to the seismo-tectonic setting, no giant earthquakes are supposed to occur in these densely populated coastal zones of Chile.

2.3 *Holocene sea level history*

A higher sea level of less than 5 m a.s.l. (above mean sea level) was suggested for Central Chile during the mid-Holocene (Ota & Paskoff 1993, Isla et al. 2012). However, considerable differences in the tectonic behavior and relative sea level history between coastal segments on a local, regional and supraregional scale must be expected (Bookhagen et al. 2006, see also Vött 2007). The differentiation of the effects of coseismic and/or postseismic tectonics (e.g. Barrientos 1995), aseismic crustal behavior and tsunami deposition as well as, in southern Chile, glacio-isostatic rebound on the one hand, and of purely eustatic changes on the other hand remains particularly difficult.

For the Bays of Tongoy and La Herradura, Ota & Paskoff (1993) assume a higher (relative) mid-Holocene sea level and a maximum of the Holocene transgression at ~6000BP. Moreover, slow coastal uplift during the Holocene is inferred based on 3000–2000 year old littoral sediments found at 3.5–5 m a.s.l. In the same area, Darwin (1846) as well as Paskoff (1973) reported on Holocene marine terrace levels below the last Interglacial terrace. Comparable conclusions are made by Encinas et al. (2006) for the Estero San Jerónimo alluvial plain near Algarrobo, south of Valparaíso. A summary of findings relevant for Holocene sea level in Chile is given in Isla et al. (2012).

As to the present conditions, the study area is characterized by a microtidal regime. Significant wave heights during storm events in the open Pacific off Chile and Peru may reach 5–6 m on average; for instance, in the period 2007–2011, a maximum significant wave height of 5.81 m was recorded (buoy 32012, National Data Buoy Center, http://www.ndbc.noaa.gov; see also Stopa et al. 2012). For the Concón Bay, situated directly south of the study area of this study, near-shore maximum wave heights are reported to be 1–3 m in general, originating from W, NW or SW wind directions (Martinez et al. 2011).

3 *Methods*

For the detection of late Holocene palaeogeographical changes and changes in coastal geomorphodynamics we performed sediment corings and used trenches to investigate the stratigraphical succession of coastal geo-archives. To assess the archives' geomorphological context, geomorphological mapping in the field (spring 2011) as well as the visual interpretation of the local geomorphology and geomorphodynamics using satellite images from 1970 (Corona satellite image, United States Geological Survey) and 2005 (Google Earth) were carried out. Elevation of cores and profiles was measured using a Topcon HiPer Pro differential global positioning system (DGPS, altimetric accuracy of ~2 cm).

Coring LSE 1 was performed by means of an Atlas Copco Cobra mk 1 percussion corer with sediment cores of 5 and 6 cm in diameter. Additionally, in the Quebrada Pachingo coastal swamp (Bay of Tongoy), one sediment core was obtained by pushing a plastic tube, 2 m long and 7.5 cm in diameter, into the sediment by hand (core TON 1). Vibracores and push cores were documented and sampled in the field, grain size distribution estimated according to Ad-hoc Arbeitsgruppe Boden (2005). For the interpretation of the sedimentary findings and to infer palaeoenvironmental and geomorphodynamic changes from the record, sedimentological, geochemical and macro- and microfaunal analyses were undertaken in the laboratory. The air-dried and hand-pestled fine-grained fraction (< 2 mm) of the samples was analyzed for Ca, Fe, Na and K concentrations using atomic absorption spectrometry (Perkin Elmer A-Analyst 300) after digestion with concentrated HCl (37 %). $CaCO_3$ was measured applying the Scheibler method, loss on ignition (LOI) determined by oven-drying at 105 °C for 12 h and ignition in a muffle furnace at 550 °C for 4 h (Beck et al. 1993). For core profile TON 1, the inorganic element composition was determined using

Tab. 1. ^{14}C-AMS dating results used for the geochronological interpretation. Notes: unid. plant remains – unidentified plant remains; unid. m. fragments – unidentified mollusc fragments. Lab. no. – Laboratory number, UGAMS = Center for Applied Isotope Studies, University of Georgia (USA). * – marine reservoir correction with 400 years. "#" – calibration yielded several possible age intervals because of multiple intersections with the calibration curve; the oldest and youngest possible ages are depicted.

Sample	Depth (m a.s.l.)	Lab. no.	Sample description	δ^{13}C (ppm)	^{14}C age (BP)	1σ max-min (cal BC/AD)	2σ max-min (cal BC/AD)
LOV 6/1	3.50	UGAMS9017	unid. m. fragments	−0.4	1560 ± 20	*792-870 AD	*#748; 905 AD
LOV 6/3	4.10	UGAMS9018	unid. m. fragments	1.3	1370 ± 20	*1007-1055 AD	*974-1103 AD
LOV 6/5	4.65	UGAMS9019	unid. m. fragments	1.1	720 ± 20	*1550-1629 AD	#*1522; 1654 AD
LSE 1/5	−1.25	UGAMS9465	unid. plant remains	−27.4	70 ± 20	#1819;1955 AD	#1714; 1955 AD
LSE 1/6	−1.35	UGAMS9466	unid. plant remains	−27.2	120 ± 20	#1711; 1952 AD	#1698; 1953 AD
LSE 1/16	−2.35	UGAMS9567	unid. plant remains	−26.0	280 ± 20	#1639; 1664 AD	#1525; 1796 AD
PCU 2/3	−0.03	UGAMS9020	organic matter	−26.5	300 ± 20	#1526; 1655 AD	#1510; 1666 AD
PCU 3/1	−0.10	UGAMS9021	unid. rhizome remain	−26.9	180 ± 20	#1675; 1950 AD	#1671; 1951 AD
PCU 3/2	−0.10	UGAMS9022	*Cyprus californicus*	−27.2	130 ± 20	#1708; 1925 AD	#1697; 1952 AD
TON 1/17	−0.17	UGAMS10625	seeds	−12.5	2290 ± 25	377-211 BC	388-204 BC
TON 1/33	−0.33	UGAMS10625	seeds	−11.7	1740 ± 45	259-420 AD	235-533 AD
TON 1/54	−0.54	UGAMS10625	seeds	−15.0	1810 ± 25	240-333 AD	176-388 AD
TON 1/63	−0.63	UGAMS9464	seeds	−7.1	1090 ± 25	991-1018 AD	#903; 1032 AD

an ITRAX X-Ray fluorescence (XRF) core scanner (Cox Analytical Systems). Semi-quantitative variations of elements from Al to U were analyzed by scanning at 1 mm resolution and an exposure time of 20 sec. Count rates (cr) represent element amounts and an estimation of the relative concentrations in the sediment. Microfossil analysis was carried out for cores TON 1 and LSE 1 in order to support textural and geochemical results, to verify the provenance of distinct sedimentary units and to determine sediment source areas. Samples (10 cm^3) were pre-treated with H_2O_2 (30 %) for dispersion and sieved to isolate fractions of > 100 and < 100 µm. The content of microfossils was investigated under a stereo light microscope and recorded quantitatively. Palaeoenvironmental interpretations are mainly based on Meisch (2000).

For the geochronological framework of coastal stratigraphies, mollusc and plant remains were dated by ^{14}C-AMS. The dating results were calibrated with CALIB 6.01 (Reimer et al. 2009) utilizing the Terrestrial (SHCal04) Southern Hemisphere calibration curves. Marine carbonates were corrected for a reservoir effect of 400 years (Reimer et al. 2009) (Table 1).

4 *Results*

4.1 *Sediment core LSE 1 (Bay of Coquimbo)*

Back-barrier estuary environments presently exist in the very northern part of the Bay of Coquimbo (Fig. 1) in the river mouth of the Quebrada de Teatinos. The sedimentary succession

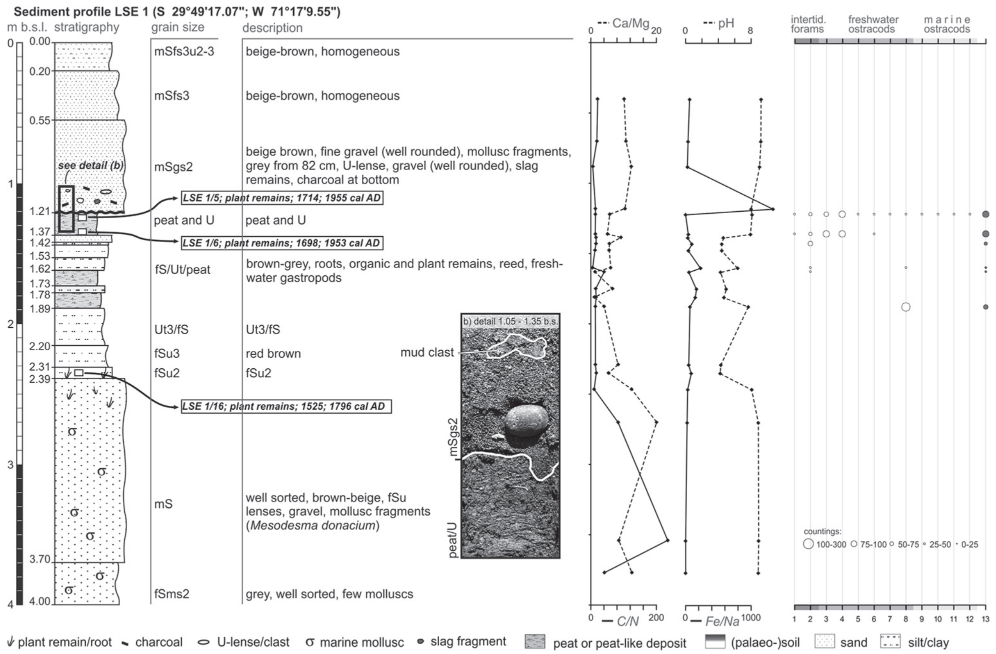

Fig. 3. Sediment core LSE 1, northern part of the Coquimbo Bay. The stratigraphical succession reflects the formation of a back-barrier coastal wetland on top of former beach sediments and indicates coastal retreat of ~400 m during the last several hundred years (see Fig. 1). A possible historical event layer (tsunami/El Niño flooding event) is visible at the top. 1 – *Trochammina inflata*; 2 – *Trochamminita irregulans*; *3 – Darwinula stevensoni*; 4 – *Penthesilenula brasiliensis*; 5 – *Pseudocandona* sp.; 6 – *Heterocypris salina*; 7 – *Sarscypridopsis aculeata*; 8 – *Cyprideis* cf. *torosa*; 9 – *Dolerocypris marina*; 10 – *Cytherura portomonttensis*; 11 – *Xestoleberis chilensis*; 12 – *Ambocythere dentata*; 13 –ostracods and foraminifers (total sum). Inlay (b) shows a detail of the boundary between the suggested event unit in the upper part of the core (above 1.21 b.s.l.) and the underlying peat.

of core LSE 1 [4.00–3.70 m below surface (b.s.), Fig. 3] starts with relatively well-sorted fine to medium sand containing mollusc remains (mainly *Mesodesma donacium*). Grain size increases to brown medium sand and gravel in the subsequent stratum (3.70–2.39 m b.s.) overlain by a unit of fine-grained sediments (silty and clayey fine sand) and three peat-like units (1.78–1.89, 1.62–1.73 and 1.21–1.37 m b.s.). Plant remains from the lower part of this unit, directly above the medium sand, were dated to 1525–1796 cal AD (sample LSE 1/16, 2.35 m b.s., Table 1). In the lowermost peat layer (c. 1.88 m b.s.), numerous specimen of the ostracods *Cyprideis* cf. *torosa* were found. While only the intertidal foraminifera *Trochamminita irregularis* and one specimen of *Cyprideis* cf. *torosa* were detected in the sediments between 1.65 and 1.37 m b.s., the foraminifera *Trochammina inflata* and freshwater ostracods (*Darvinula stevensoni*, *Penthesilenula brasiliensis*, *Heterocypris salina*) additionally occur in the subsequent sample LSE 1/6 (1.36 m b.s.). Above (sample LSE 1/5, 1.22 m b.s.), a considerable increase in microfaunal diversity is observed, comprising the intertidal foraminifers *Trochamminita irregularis* and *Trochammina inflata*, several freshwater ostracods (*Darwinula stevensoni*, *Penthesilenula brasiliensis*, *Pseudocandona* sp., *Heterocypris salina*, *Sarscypridopsis aculeata*) as well as several marine ostracods (*Dolerocypris marina*, *Cytherura portomonttensis*, *Xestoleberis chilensis*, *Ambocythere den-*

tata). The uppermost peat layer (1.21–1.37 m b.s.) was dated to between 1698–1953 cal AD (LSE 1/6) and 1714–1955 cal AD (LSE 1/5) (Table 1). On top of the peat, a sandy unit occurs, consisting of medium and coarse sand in its lower part, and medium and fine sand in its upper part. At its base, well rounded gravel and mollusc remains, charcoal and slag fragments as well as mud clasts were found. No microfauna were detected.

4.2 *Sediment core TON 1 (Quebrada Pachingo, Bay of Tongoy)*

In the Bay of Tongoy, ~50 km south of Coquimbo, back-barrier and partly swampy coastal lowlands are present in three river mouth areas (Fig. 1). In the westernmost coastal swamp, the Quebrada Pachingo river mouth (Figs. 1 and 4), a push core (TON 1, Fig. 5) was obtained from its eastern part, some 200 m from the present beach.

The lower Quebrada Pachingo river channel interrupts a system of beach ridges stretching from the cliffs of the last Pleistocene marine terrace (elevation ~20 m a.s.l., RADTKE 1987) to the present coastline (elevation of youngest ridge ~2–3 m a.s.l., OTA & PASKOFF 1993). According to OTA & PASKOFF (1993), beach ridges c. 300 m from the coast formed later than c. 2000–2200BP, and the most seaward ridge contains mollusc remains dating to c. 500 BP (recalibrated ages). According to the interpretation of satellite images, Aster DEM and SRTM data, channel incision and lateral erosion has formed oxbow-shaped structures at several places (Fig. 4). Different levels of fluvial terraces are distinguished, separated by the undercut slopes of the next, younger generation of channel incision.

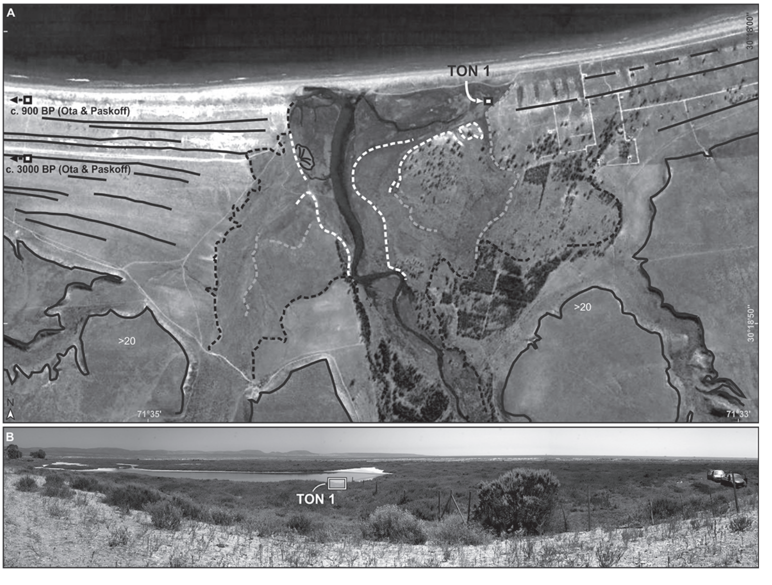

Fig. 4. (A) Setting of the study site at Tongoy Bay, Quebrada Pachingo river mouth. Channel incision and lateral erosion have formed oxbow-shaped structures at several places (marked by dotted lines). Different terrace levels with different elevations can be distinguished, separated by the undercut slopes of the next, younger generation of channel incision (image based on Google earth). (B) Panorama photo of coring site TON 1 as seen from southward lying beach ridge remnants.

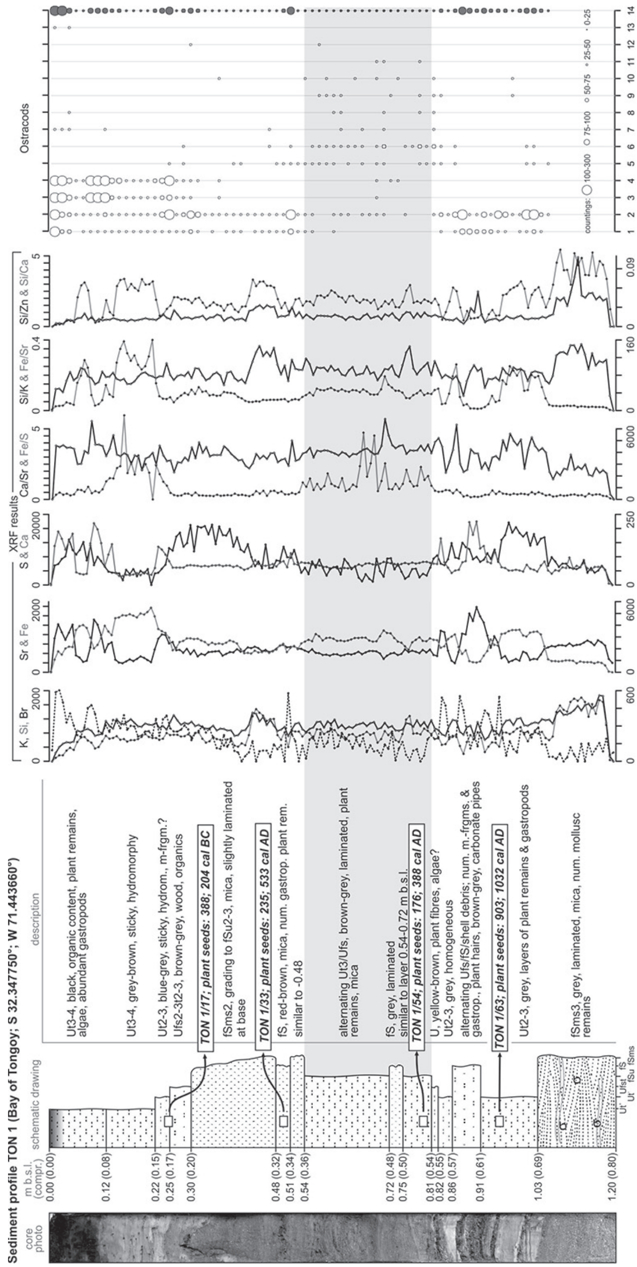

Fig. 5. Sediment core TON 1 with dating results. The sequence of 120 cm is indicated by an alternation of silty and sandy units. Microfaunal analyses document a trisection, beginning with a brackish environment at the base, a subsequent sudden occurrence of freshwater conditions (grey shaded section) and a following gradual transition to recurrent brackish environments. 1 – *Cyprideis cf. torosa*, 2 – *Cyprideis cf. torosa* juv., 3 – *Sarscypridopsis aculeata*, 4 – *Sarscypridopsis aculeata* juv., 5 – *Heterocypris salina*, 6 – *Heterocypris salina* juv., 7 – *Ilyocypris* sp., 8 – *Ilyocypris* sp. juv., 9 – *Dawinula stevensoni*, 10 – *Herpetocypris* sp., 11 – *Potamocypris unicaudata*, 12 – *Cypridopsis* sp., 13 – *Leptocythere* sp., 14 – ostracods (total sum).

Tab. 2. Ostracod and foraminifera species found within this study and their environmental characteristics.

Ostracods			
Species	**Nr. (Figs. 3, 5)**	**Description**	**Environment**
Ambocythere dentata	12 (3)	Hartmann 1962	marine
Cyprideis cf. *torosa*	1, 2 (5) 8 (3)	Jones 1850	Brackish waters, fluctuating salinity, broad range of salinity, optimum at 2–16 ‰, generally in brackish water bodies
Cypridopsis sp.	12 (5)		Freshwater
Darwinula stevensoni	9 (5) 3 (3)	Brady & Robertson 1870	Freshwater to slightly saline standing water bodies, lakes and slow flowing waters; salinity up to 15 ‰
Cytherura portomonttensis	10 (3)	Hartmann 1962	Marine, littoral
Dolerocypris marina	9 (3)	Hartmann 1965	Marine, sandy silt
Herpetocypris sp.	10 (5)		Freshwater
Heterocypris salina	5, 6 (5) 6 (3)	Brady 1868	Freshwater to slightly saline water bodies, also in freshwater; common in coastal waters, optimum at 5–10 ‰ and 15 °C (Ganning, 1967); often together with other halophylic ostracods, e.g. *Sarscypridopsis aculeata*, *Potamocypris unicaudata*
Ilyocypris sp.	7, 8 (5)		Freshwater to slightly saline water bodies
Leptocythere sp.	13 (5)		Marine, also migration to brackish coastal water bodies (Horne et al. 2001)
Penthesilenula brasiliensis	4 (3)	Pinto & Kotzian 1961	Freshwater
Potamocypris unicaudata	11 (5)	Schäfer 1943	Freshwater and slightly brackish standing and flowing water bodies; salinity 0,1–4,2 ‰; common in slightly brackish coastal waters; together with *Heterocypris salina* and/or *Sarscypridopsis aculeata*
Pseudocandona sp.	5 (3)		Freshwater
Sarscypridopsis aculeata	3, 4 (5) 7 (3)	Costa 1847	Mainly in freshwater to slightly brackish water bodies, permanent and temporary/periodical water bodies, lower salinity tolerant than *C. torosa*; optimum at 5 and 10 ‰; often together with *Heterocypris salina*
Xestoleberis chilensis	11 (3)	Hartmann 1962	Marine
Foraminifers			
Species	**Nr. (Fig. 3)**	**Description**	**Environment**
Trochammina inflata	1 (3)	Montagu 1808	Intertidal foraminifer
Trochamminita irregularis	2 (3)	Cushman & Brönnimann 1948	Intertidal foraminifer

Fig. 6. Panorama photo of the setting of study sites at Pichicuy and Los Vilos. (A) The Bay of Pichicuy as seen from the Panamerican Highway (Panamericana at Puente Huaquén). Trench PCU 2 (Fig. 8) is located on a low-lying terrace, formed by subrecent channel incision. (B) Coastal setting at sampling site LOV 6; the profile is situated c. 50 m from the present beach (see Fig. 7). The natural outcrop formed due to lateral erosion of the depositional beach sediment sequence.

At coring site TON 1, taken approximately from the elevation of the present estuary, the sedimentary record of the upper 120 cm is a sequence of alternating silty and sandy deposits. The sand unit at the base of the sedimentary succession (1.20–1.03 m b.s.) is void of ostracods. Macroscopic mollusc remains comprise *Protothaca* sp. and *Mactra* sp. Subsequently, silty to clayey deposits accumulated at site TON 1. Here, numerous specimens of *Cyprideis* cf. *torosa* are present, showing large numbers of juvenile individuals in several sections. Few individuals of *Heterocypris salina* were found as well. Above 0.81 m b.s., a slight lamination of the deposit is visible, reflecting alternating thin layers of clayey and fine sandy silt. Generally, grain size slightly increases upwards and mica minerals are visible, the latter corresponding to high Si values (reflected in Si/K, Si/Zn and Si/Ca ratios). Between 0.75 and 0.72 m b.s., a well-defined fine sand layer occurs. Together with the sedimentary changes (lamination), the ostracod assemblage changes as well (Fig. 5). While only very few or no individuals of *Cyprideis* cf. *torosa* are present, different species (*Heterocypris salina*, *Iliocypris* sp., *Dawinula stevensoni*, *Herpetocypris* sp., *Potamocypris unicaudata*; see also Table 2) characterise the different sedimentary units up to c. 0.54 m b.s., generally reflecting a higher diversity. With the beginning of the unit of fine to medium sand at 0.54 m b.s., diversity again decreases between 0.54 and 0.30 m b.s.; here, *Cyprideis* cf. *torosa* is present in low numbers, and the species *Iliocypris* sp., *Dawinula stevensoni*, *Herpetocypris* sp. and *Potamocypris unicaudata* disappear above c. 45 cm b.s. Subsequently, comparable to the sediments between 1.03 and 0.81 m b.s., the amount of *Cyprideis* cf. *torosa* increases, but high numbers of *Sarscypridopsis aculeata* are present as well; the latter species is dominant for the upper 30 cm of the core, and several sections are indicated by high numbers of juvenile species.

As Fig. 5 shows, high Sr and low Fe values characterise the lowermost sand unit. In the subsequent sedimentary units, several units are indicated by high, others by a low Fe/Sr ratio, resulting

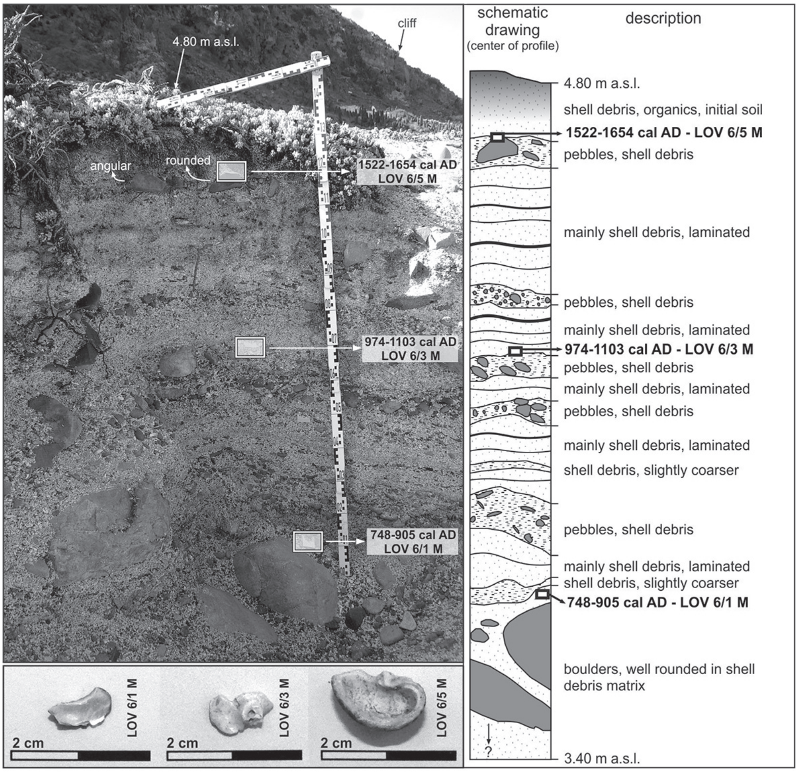

Fig. 7. Sediment profile LOV 6 and ^{14}C-AMS ages. The stratigraphy of LOV 6 consists of more than 14 layers of shell debris, gravel and sand. Accumulation of shell material terminated at around or later than 1522–1654 cal AD.

from generally inverted Fe and Sr contents in the sediment. These fluctuations seem not to be related to grain size changes only, since these are observed between units of similar grain size as well (e.g. in the upper core part at 0–22 cm b.s.). In the middle part of the core (81–22 cm b.s.), remarkable fluctuations are absent, but the Fe content decreases between 54 and 40 cm.

Larger fluctuations are shown by the Br values; while the lowermost sand is indicated by relatively low contents, higher values were measured in the overlying fine grained sediments. Above 81 cm b.s., lower values characterise the middle part of the core, but values gradually increase above 40 cm b.s. and stay relatively high in the upper part of the core. In the fine sand layer at 51–48 cm b.s., Br contents are remarkably high. Again, no distinct correlation with grain size is observed.

For the Ca values, a correlation with the total abundance of ostracods is inferred; where microfossil content is high, Ca values also increase (Fig. 5). In contrast, S values show increasing values between 1.03 and 0.81 m b.s.; sediments above 81 cm b.s. are indicated by lower contents, but, similar to the Br values, a gradual increase is observed between 0.54–0.30 cm b.s. In the upper part of the core, S values again decrease above 0.30 cm b.s., before increasing to the top.

Four ^{14}C-AMS datings of seed remains yielded – from bottom to top – ages of 903–1032 cal AD (TON 1/63), 176–388 cal AD (TON 1/54), 235–533 cal AD (TON 1/33) and 388–204 cal BC (TON 1/17), documenting an apparent age inversion (see Table 1).

4.3 *Sediment profile LOV 6 (Los Vilos)*

Sediment profile LOV 6 (Fig. 7, see also Figs. 1 and 6) is situated some 2.6 km south of Los Vilos and some 500 m south of the Quebrada Quereo (see VILLAGRÁN & VARELA 1990, NUÑEZ et al. 1994). The coastal setting is characterised by narrow pocket beaches, laterally separated by cliff remnants and landwards bordered by a ~10 m high cliff (Figs. 1 and 7).

The profile consists of a sequence of at least 14 sedimentary layers, mainly composed of shell debris, sand and gravel. The majority of the shell content appears to be subangular, but angular fragments occur as well. Some of the stratigraphical layers contain coarser material up to the size of boulders (maximum size about 40 cm) – this is particularly the case for the lowermost layer of the profile, where large clasts are incorporated in the horizon. Most of these coarse components are well rounded, though, in some layers, and in particular on top of the uppermost horizon, angular fragments of the adjacent cliff are present. On top of the uppermost horizon, a weak soil has developed, indicated by organic components as well as a darker colour in the first centimetres below the surface.

Three mollusc samples from three different shell debris layers were ^{14}C-dated, all of them being characterised by angular edges in order to avoid age inversions due to reworking. The results are consistent with the stratigraphic sequence: 748–905 cal AD (LOV 6/1 M), 974–1103 cal AD (LOV 6/3 M) and 1522–1654 cal AD (LOV 6/5 M).

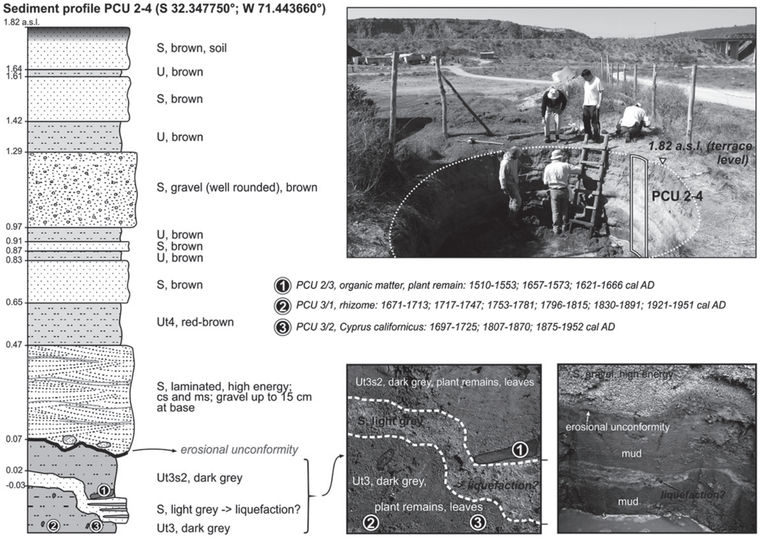

Fig. 8. Sediment profile PCU 2 with ^{14}C-dated samples. The assumed liquefaction layer shows interfingering with the surrounding mud unit and is younger than ~1697AD.

At present, the deposits building up the sedimentary succession of profile LOV 6 are being eroded; no accumulation of further shell debris layers takes place at this site.

4.4 *Sediment profile PCU 2 (Bay of Pichicuy)*

Sediment profile PCU 2 (Fig. 8, see also Figs. 1 and 6) was performed in an artificial well-like excavation and is located in the Bay of Pichicuy, some 20 km northwest of the city of La Ligua. The profile's surface is situated at ~1.80 m a.s.l. on top of the lowest fluvial terrace level, resulting from incision of the Quebrada Pichicuy. At the very base, below the visible part of the outcrops, heterogeneous, poorly sorted sand was found. On top of the sand, a fine-grained unit of clayey to sandy silt is present all along the outcropping sediments in the trench indicating a quiescent, swampy depositional environment. Several root and other plant remains of, for instance, *Cyprus californicus* occur in this unit. Intercalating the mud facies, at a depth of c. 1.90 m b.s., a sandy layer was found, showing a remarkable variability in thickness and an undulating topography. At some places, the sand layer splits into several thin sand layers interfingering with the surrounding mud. Its grain size is similar to the unit underlying the mud.

On top of the silty mud unit, a sand layer is present, characterised by a sharp erosional contact at its base. Alternating layers of sand and silt follow towards the top of the profile. From the basal mud unit, three ^{14}C-AMS datings gave ages between 1515 and 1953 cal AD (PCU 2/3: 1510–1666; PCU 3/1: 1671–1951; PCU 3/2: 1697–1952) (Table 1).

5 *Discussion – coastal changes and palaeoseismological implications*

5.1 *Coastal changes in the N Coquimbo Bay*

5.1.1 *Environmental changes inferred from sedimentological and microfaunal findings*

Beach aggradation is inferred from sublittoral and littoral sediments [well sorted medium to gravelly medium sand, mollusc remains of littoral origin (*Mesodesma donacium*)] found in the lower part of core LSE 1. Silty and clayey strata as well as peat sequences covering the littoral sediments document the onset of back-barrier depositional environments at around 1600–1800AD (LSE 1/16, 1525; 1796 cal AD). Two peat samples taken from the upper part of this sequence show slightly younger ages and reflect prevailing back-barrier environments, possibly until the 19th or even 20th century (LSE 1/5 PR, LSE 1/6 PR).

The microfaunal analyses suggest brackish, intertidal environmental conditions (*Trochamminita irregularis*, *Cyprideis* cf. *torosa)* during deposition of these sediments, but increased freshwater influence in the upper part of the sequence is attested by the ostracods (Fig. 3). However, the microfaunal assemblage shows both marine and freshwater indicators in the uppermost part of the back-barrier sediments (LSE 1/5), pointing to increased saltwater influence in the estuary system. Since no changes of the depositional environment can be inferred from the sedimentary findings, this microfaunal assemblage may have been induced by an intermittent opening of the sand barrier closing the estuary, or by altered circumstances of the groundwater zonation (e.g. by local tectonics), rather than by an extreme wave event.

5.1.2 *A (sub) recent event layer in N Coquimbo Bay*

According to the characteristics of the following sand unit in profile LSE 1, indicated by an erosive contact to the underlying mud, mud clasts, and basal gravel components, the interruption of back-barrier depositional conditions by sandy deposits suggests a high-energy flooding event which seems to have affected the coastal marsh along the lower Quebrada Teatinos. No microfaunal remains were found in this sandy unit and the poor preservation of the few macrofaunal remains hindered the determination of species.

Given its sedimentological characteristics, the deposition of this stratum may result either from (i) a remarkable flood event of the Teatinos River, or from (ii) a tsunami event, assuming that the source of the sediment (in this case probably sublittoral to littoral sediments) is poor in microfauna. The dating results are unable to accurately determine the age of the suggested event due to ^{14}C age plateau problems (Reimer et al. 2009, Williams 2012) and related multiple possible age ranges of the calibrated ^{14}C results. Deposition may have taken place shortly after 1714AD, but also shortly after 1955AD. Historical records point to a major flooding of the Teatinos River, such as the one in March 1856 (Vicuña-Mackenna 1877: 315, Bahre 1979) or other large discharge events, probably linked to strong El Niño conditions in the area (e.g., Gergis & Fowler 2009, Ortega et al. 2012). This assumption is supported by high Fe content at the base of the event deposit (Fig. 3) that contrasts with the low Fe content of the inferred littoral deposits at the base of the core. Indeed, the high Fe values probably reflect the influence of the iron mine El Romeral located upstream of the coring site, which was established at the beginning of the 20th century. Fe-rich particles, transported from upstream by fluvial discharge, were re-deposited by the event and particularly accumulated in the lower part of the event's deposit due to density segregation.

Besides major flooding of the river mouth area by exceptional discharge events, several tsunami events may be considered as potential triggers for the deposition of the upper sandy unit as well. First, the 1730 Great Valparaíso Earthquake is reported to have caused a strong tsunami along the Central Chilean coast (Lomnitz 2004). Second, a further strong tsunami took place in 1922, following a magnitude 8.4 earthquake near Copiapo (epicenter off Huasco-Vallenar). During this tsunami, run-up is reported to have exceeded 7 m at Coquimbo in the southern part of the bay. Further possible tsunamis occurred in relation to earthquakes in 1819 (M_w 8.5, Copiapo), 1849 (M_w 7.5, Coquimbo; ~5 m above high water mark in Coquimbo bay) and in 1868 (M_w 8.5, Arica). The ^{14}C age of sample LSE 1/16 (1525; 1796 cal AD) determines the beginning of back-barrier environments at site LSE 1 to sometime before or during 1525–1796 cal AD. Based on the subsequent accumulation of more than one meter of fine grained, muddy sediments and three peaty layers during back-barrier conditions, we assume that the suggested event is rather related to a younger event – such as the 1922 tsunami or, more likely, a large flooding event during El Niño conditions such as in 1856 (Gergis & Fowler 2009).

5.1.3 *Potential tectonic influence during historical times?*

In general, the sedimentary sequence of LSE 1 clearly indicates remarkable coastal changes in the northern part of the Bay of Coquimbo during the last ~400 years. Beach aggradation resulted in a seaward coastal progradation of ~400 m during this relatively short period of time. As a consequence, several beach and dune ridges to the south of LSE 1 must have formed during that time as well (see Fig. 1). These findings point to high coastal dynamics and a general adjustment to new geomorphodynamic conditions. Moreover, in contrast to the long-term uplift trend documented by the flight of Pleistocene marine terraces (and late Holocene marine sediments at 3–5 m a.s.l.) in the adjacent areas (LEONARD & WEHMILLER 1992, OTA & PASKOFF 1993), tectonic subsidence may be inferred from the elevation of the back-barrier swamp in core LSE 1 (~1.20 m b.s.l.; below mean sea level) dated younger than 300 yrs. According to the age range of the lowermost sample (LSE 1/16: 1525; 1796 cal AD), core LSE 1 records remarkable coastal changes during the last ~400 years, potentially triggered by accompanied vertical tectonics. Thus, a relation to the Great Valparaíso Earthquake in 1730 may be suggested.

5.2 *Geomorphodynamic changes in the Bay of Tongoy*

5.2.1 *Environmental changes as derived from ostracod taxa and geochemistry*

At the base of core TON 1, the sandy unit between 1.20 and 1.03 m b.s. is interpreted to represent sublittoral deposits. Relatively high Sr values in relation to Ca support this interpretation since integration of Sr and Mg in calcareous mollusc tests is favored in the marine realm (BORREMANS et al. 2009, DUEÑAS-BOHÓRQUEZ et al. 2009). According to the findings from OTA & PASKOFF (1993), presenting ^{14}C ages from the most seaward beach ridge to the west of the coring site (Fig. 4), a seaward coastal shift of ~100 m took place later than ~1450 cal AD (~500 cal BP; recalibrated ^{14}C age). This is in accordance with the findings from core TON 1, where back-barrier conditions are assumed to have started later than ~1000BP (TON 1/63, 903; 1032 cal AD). Given that the available dating results from TON 1 reflect an apparent age inversion (Fig. 5), reworking of the dated seed remains has to be considered. This is also true for the youngest and lowermost sample. However, this youngest age from the base determines the maximum age of the subsequent sedimentary sequence. The overlying strata are thus suggested to be younger than ~1000BP, resulting from a local retreat of the sea to the coastline's present position.

Based on variations in the occurrence of ostracod taxa as well as geochemical and sedimentary evidence (Fig. 5), fluctuations of environmental conditions are inferred from the following sedimentary sequence at coring site TON 1. During that time, a coastal brackish water body characterised the river mouth of the Quebrada Pachingo, influenced by both fluctuating marine (saltwater) and fluvial (freshwater) input. Although the ostracod assemblage generally reflects a brackish environment until 81 cm b.s., variations in the geochemical composition (e.g. S, Fe, Sr) point to a changing chemistry of the water body or the sediment composition. Elevated S and Fe values suggest anoxic conditions, favorable to pyrite formation (at 103–95 cm b.s.). Due to elevated amounts of siliciclastic components at the base of the laminated section at 91–86 cm b.s., subsequent fluvial deposition may be inferred. Increasing Fe contents towards the top of this layer in turn may reflect subaerial conditions. Locally, distinct peaks in Br point to a high organic content, i.e. swamp-like conditions.

At some time after ~900–1000AD a freshwater habitat established. The ostracod assemblage above 81 cm b.s. consists of *Heterocypris salina*, *Ilyocypris* sp., *Dawinula stevensoni*, *Herpetocypris* sp. and *Potamocypris unicaudata*, suggesting a rapid alteration of environmental conditions. This freshwater-influenced section clearly shows increased Fe/S values, pointing to reduced S as an effect of weakened saltwater influence. In particular, the sandy section above 48 cm b.s. points to a temporarily increased siliciclastic input. Elevated S values towards the top of this unit may reveal gradually increasing salinity, culminating in the re-establishment of brackish conditions (represented by *Cyprideis* cf. *torosa* and *Sarscypridopsis aculeata*).

Fluctuating environmental conditions are reflected by ostracods and geochemistry in the uppermost part of the core as well (0.30–0 m b.s.). Although no distinct fluvial input is evidenced by grain size or geochemical characteristics, the period of overall brackish conditions was interrupted twice, at c. 22–14 cm and 8–5 cm b.s. In addition to inappropriate conditions for brackish ostracod assemblages, low S and high Fe contents to the top rather indicate here a temporary increase of freshwater influence and a temporary subaerial exposure than anoxic conditions and pyrite production. Similar conditions prevail at the present surface.

In summary, cycles of changing environmental conditions have occurred at coring site TON 1 throughout the past several hundred years. Temporary subaerial (no water coverage, oxidation) and/or freshwater dominance is indeed deduced for parts of the upper and middle core section. Possible causes for the environmental changes in the coastal marsh of the Quebrada Pachingo are (i) coseismic coastal uplift and the sudden reduction of saline groundwater input to the coring site; (ii) fluvial input due to flooding events or channel shifting; or (iii) climatically-induced lowering of the water table, at least for the fluctuations in the upper core section (dry conditions, increased evaporation).

5.2.2 *Indications for tectonic influence in the recent past*

As for the distinct shift of the ostracod assemblage to freshwater-preferring species in the middle core part (81–54 cm b.s.), comparable findings are reported from the Cascadia subduction zone (NW America) and from Japan (Sawai 2001, Hawkes et al. 2005, 2011). In these cases, the microfaunal change is related to tectonic subsidence. Tectonic uplift of the coastal plain may thus be inferred from the change of brackish to freshwater-dominated conditions in the middle part of the core. While vertical tectonic movements generally were highlighted in the study area (Radtke 1987, Saillard et al. 2009, Pfeiffer et al. 2011), the overall uplift trend during the Holocene is estimated to be relatively low (1.6 m/ka, Saillard et al. 2009; 0.1–0.2 m/ka, Ota & Paskoff 1993) when compared to other coastal sections in Central Chile.

However, the observed environmental changes in the middle part of the core may also be explained by the onset of fluvial activity at coring site TON 1, accompanied by a temporary shift of the main river channel. This interpretation is supported by the ostracod assemblage, pointing to a freshwater-dominated environment and low flow velocity (*Heterocypris salina*, *Darwinula stevensoni*, *Potamocypris unicaudata*; Table 2). The presence of visible mica minerals and siliciclastic material in the related sediments (Fig. 5) reflects the clastic input from the Quebrada Pachingo's catchment.

Different terrace levels in the lower Quebrada Pachingo area are evidence of several incision periods of the torrential Pachingo river into its own sediments and beach ridge sequences of, according to the mollusc age presented by Ota & Paskoff (1993), mid- to late Holocene age. We thus suggest that repeated tectonic uplift of the coastal segment during the Holocene, inducing almost continuous channel adjustment to base level changes, triggered these incision events, in most cases accompanied by lateral channel migration. Indeed, Ota & Paskoff (1993) infer a slow uplift in the Bays of Tongoy and La Herradura during the Holocene from 3000–2000 year old littoral sediments (i.e. 3000 years younger than the inferred sea level high stand/transgression maximum) found at 3.5–5 m a.s.l., corroborating the observations of repeated river incision and the inferred uplift presented in this study. The inferred shift of the main estuary river channel to coring site TON 1 thus may have been induced by vertical tectonics as well, with the consequence of channel adjustment to different base levels in the lower Quebrada area.

In the given case, the dating results may suggest the influence of a seismic event later than c. 1000AD, related to coastal uplift. However, all ^{14}C ages above the sediment layer of sample TON 1/63, for which a maximum age of ~1000AD may be deduced, are older. This suggests a remarkably long reworking time of the dated seeds. Thus, historical seismic events may have been responsible for either the distinct shift to freshwater-dominated conditions in the middle part of the core or for the inferred temporarily subaerial conditions in the upper part of the core. Whether these changes were due to post- or coseismic tectonics remains an open question.

5.3 *Geomorphodynamic changes south of Los Vilos*

According to the findings from sediment profile LOV 6 (Los Vilos) in the southern part of the study area, the accumulation of shell debris layers and well-rounded gravel and boulders suggests a dynamic and stepwise deposition of beach sediments at least throughout ~850 years (Table 1, Fig. 7). Assuming that we reached the base of these deposits, these conditions started at ~1200BP (LOV 6/1 M, 748–905 cal AD; Table 1, Fig. 7). On the top of the sequence, in the uppermost shell-debris layer, we note the development of an initial soil and the accumulation of scattered cliff material. According to these results, we interpret the sequence as beach environments affected by persistent storm conditions until 1522–1654 cal AD (LOV 6/5 M), when suddenly littoral dynamics and accumulation of shell material and well-rounded pebbles ceased.

Again, we observe a considerable change in coastal geomorphodynamics possibly around the beginning of the 17th century, associated to a shift from accumulation to erosion. This shift may indeed be explained by sudden uplift of the sedimentary sequence, which stopped the accumulation of well-rounded littoral pebbles and shell debris.

5.4 *Possible liquefaction and historical coastal uplift in the coastal plain of Pichicuy Bay*

The sand layer intercalating the basal mud sediments of profile PCU 2 between 0.03 m b.s.l. and 0.02 m a.s.l. (Fig. 8) may be interpreted as a liquefaction feature, based on its (i) undulating topography; (ii) similar grain size compared to underlying strata; (iii) distinct interfingering with mud, although no dikes or volcanoes were detected along the outcrop. Liquefaction occurs during earthquakes of considerable magnitude, depending on the distance to the epicenter and earthquake parameters such as shaking duration or frequency wave trains (Galli 2000). The ground shaking effects can lead to the injection of underlying sand into the overlying mud sediments, caused by increased pore-water pressure and following liquefaction of the saturated cohesionless sediment (Youd 1977, Guarnieri et al. 2009). However, sand dikes or sand volcanoes, reported to be reliable criteria for this interpretation (Martin & Bourgeois 2012), were not found in the investigated trench PCU 2. Likewise, tsunami events may deposit thin sand sheets in coastal swamp deposits, leaving comparable sand layers in mud stratigraphies. However, a marine flooding origin of the sand sheet remains ambiguous, since no carbonate contents, i.e. marine faunal elements, or typical sediment structures such as fining-up sequences or erosive contacts were detected.

The stratigraphy and chronology from sediment profile PCU 2 furthermore reminds of the previously discussed scenario at Coquimbo Bay. We observe the deposition of organic-rich mud sediments, subsequently eroded during the deposition of the younger fluvial sandy unit (Fig. 8). Similar to the findings at LSE 1, a major discharge event related to strong El Niño conditions may have triggered the deposition of this sand unit (Gergis & Fowler 2009).

As for the age of the assumed liquefaction unit, it is not clear whether the sand injection occurred during the existence of the swamp and prior to the deposition of the overlying sand unit, or subsequent to the deposition of the fluvial deposits found above 0.07 m a.s.l. (Fig. 8). Also, the ^{14}C age plateau once again hinders a precise age determination (Reimer et al. 2009). At 1666 cal AD (minimum age; PCU 2/3), a coastal swamp existed at location PCU 2. Sample PCU 3/2 gives a maximum age of 1697 cal AD (i) for the assumed liquefaction unit, and (ii) for the deposition of the overlying fluvial sediments and the subsequent fluvial incision (cf. Figs. 6 and 8). If the sand injection took place subsequent to the deposition of the fluvial sequence, one single main seismic event could be responsible for (i) the formation of the assumed liquefaction unit, (ii) the coastal uplift and (iii) the subsequent river incision. However, between 1700 and 1950AD, numerous strong earthquakes are reported and may have been responsible for this sequence of processes. A possible candidate is the 1730 Great Valparaíso Earthquake that affected a long segment or several segments of the megathrust. Other candidates are events reported to have affected smaller segments of the subduction zone than the 1730 earthquake, such as in 1822 (M_w 8–8.5, Valparaíso/La Ligua; coastal uplift 1–2 m), 1847 (M_w 7, La Ligua), 1850 (M_w 7.5, Casablanca), 1880 (M_w 7.5, Illapel and Petorca), 1906 (M_w 8.6, Valparaíso; coastal uplift up to 80 cm) and 1943 (M_w 8.3, Illapel). It is, however, still possible that our findings entail two or more events.

6 *Conclusions*

The presented findings reflect different aspects of coastal changes along the Central Chilean coast. At four different locations between La Serena and Papudo/La Ligua (29° 50' – 32° 20' S), a ~300 km-long coastal segment, coeval geomorphodynamic (Coquimbo Bay) and palaeoenvironmental (Bay of Tongoy) changes were identified in estuary systems, coastal swamps and coastal plains. These findings are interpreted to represent indirect evidence for palaeoseismicity affecting the coastal system by vertical tectonic movement on a regional scale.

Direct evidence for mid- to late Holocene tectonics is inferred from (i) the uplifted pocket beach (South of Los Vilos), and (ii) estuary terraces and river incision (Bay of Tongoy, Pichicuy). Moreover, a sand sheet intercalating organic mud sediments in the coastal stratigraphy at Pichicuy is assumed to represent a liquefaction unit rather than a tsunami deposit, reflecting a strong seismic event in the area.

Although the interpretation of existing ^{14}C age estimates and a linking to certain events is hindered by radiocarbon dating plateau problems, all presented ages suggest a change of coastline elevation, morphodynamic activity and/or coastal environments during the last 300 years. Similarly, the potential liquefaction sand layer dates to the same time period. The Bay of Tongoy represents the only study area where the presented dating results may allow a relation to older events, but uncertainties remain due to probable reworking of the dated seed remains.

Moreover, the back-barrier stratigraphies recorded in core LSE 1 and profile PCU 2 reflect the deposition of high-energy event deposits eroding basal organic mud sediments since the 18th century. Major flooding events related to strong El Niño conditions are assumed to be the most plausible triggering process in both cases, illustrating the potential of coastal archives for studying historic El Niño occurrence in Central Chile.

Based on the results presented here, we additionally assume that the coastal environment, geomorphology and stratigraphy are strongly influenced by tectonic processes in the study area, considerably affecting coastal or near-coastal processes and environments. However, it remains unclear whether one event or several events are responsible for the detected changes. We assume a relation to the 1730 Great Valparaíso Earthquake. If this can be confirmed – especially the relation between the 1730 event and the results from Coquimbo Bay and the Bay of Tongoy – our findings may contribute to a better understanding of the palaeoseismicity of Central Chile, and in particular the size of the ruptured segment during the 1730 Great Valparaíso Earthquake.

In general, more detailed follow-up studies on geomorphological, palaeoenvironmental and coastal dynamic changes, combined with sedimentological studies on palaeoevent deposits, may allow for estimating earthquake magnitudes, notably by providing information about the length of rupture zones.

Acknowledgements

This study was funded by the German Research Foundation (DFG ref no: BR 877/29-1) which is gratefully acknowledged. We thank Marco Cisternas (Pontificia Universidad Catolica de Valparaíso, Chile) for logistic support in the field and following discussions. Critical comments on an earlier draft of the manuscript by Max Engel (Institute of Geography, University of Cologne) considerably helped to improve the paper. Jean-Pierre Francois (Seminar für Geographie und ihre Didaktik, University of Cologne) is thanked for improving the manuscript as well. We appreciate Juliane Scheder's assistance concerning the microfaunal analysis.

References

Ad-hoc-Arbeitsgruppe Boden der Staatlichen Geologischen Dienste und der Bundesanstalt für Geowissenschaften und Rohstoffe (ed.) (2005): Bodenkundliche Kartieranleitung. – 5. Auflage, Stuttgart.

Arana, D. B. (2009): Historia general de Chile IV. – Bookmasters Inc., 440 pp.

Atwater, B. F. (1987): Evidence for Great Holocene Earthquakes Along the Outer Coast of Washington State. – Science **236:** 942–944.

Atwater, B. F., Tuttle, M., Schweig, E. S., Rubin, C. M., Yamaguchi, D. K. & Hemphill-Haley, E. (2004a): Earthquake recurrence inferred from paleoseismology. – Develop. Quatern. Sci. **1:** 331–350.

Atwater, B. F., Furukawa, R., Hemphill-Haley, E., Ikeda, Y., Kashima, K., Kawase, K., Kelsey, H. M., Moore, A. L., Nanayama, F., Nishimura, Y., Odagiri, S., Ota, Y., Park, S.-C., Satake, K., Sawai, Y. & Shimokawa, K. (2004b): Seventeenth-century uplift in eastern Hokkaido, Japan. – The Holocene **14** (4): 487–501.

BAHRE, C. J. (1979): Destruction of the Natural Vegetation of North Central Chile. – Geography **23:** 128 pp., Univ. Calif. Press, Berkeley, USA.
BARRIENTOS, S. E. (1995): Dual seismogenic behaviour – the 1985 central Chileearthquake. – Geophys. Res. Lett. **22** (24): 3541–3544.
BARRIENTOS, S. E. (2007): Earthquakes in Chile. – In: MORENO, T. & GIBBONS, W. (eds.): The Geology of Chile: 263–288, Geol. Soc., London.
BARRIENTOS, S. E., VERA, E., ALVARADO, P. & MONFRET, T. (2004): Crustal seismicity in Central Chile. – J. South Amer. Earth Sci. **16** (8): 759–768.
BECK, R., BURGER, D. & PFEFFER, K.-H. (1993): Laborskript. – Kleinere Arbeiten aus dem Geographischen Institut der Universität Tübingen, **11**.
BECK, S., BARRIENTOS, S., KAUSEL, E. & REYES, M. (1998): Source characteristics of historic earthquakes along the Central Chile subduction zone. – J. S. Amer. Earth Sci. **11** (2): 115–129.
BERNINGHAUSEN, W. H. (1962): Tsunamis reported from the west coast of SouthAmerica 1562–1960. – Bull. Seismol. Soc. Amer. **52** (4): 915–921.
BILEK, S. L. (2010): Seismicity along the South American subduction zone: Review of large earthquakes, tsunamis, and subduction zone complexity. – Tectonophysics **495:** 2–14.
BOOKHAGEN, B., ECHTLER, H. P., MELNICK, D., STRECKER, M. R. & SPENCER, J. Q. G. (2006): Using uplifted Holocene beach berms for paleoseismic analysis on the Santa María Island, south-Central Chile. – Geophys. Res. Lett. **33** (15): L15302.
BORREMANS, C., HERMANS, J., BAILLON, S., ANDRE, L. & DUBOIS, P. (2009): Salinity effects on the Mg/Ca and Sr/Ca in starfish skeletons and the echinoderm relevance for paleoenvironmental reconstructions. – Geology **37:** 351–354.
BRILL, D., BRÜCKNER, H., JANKAEW, K., KELLETAT, D., SCHEFFERS, A. & SCHEFFERS, S. (2011): Potential predecessors of the 2004 Indian Ocean Tsunami – Sedimentary evidence of extreme wave events at Ban Bang Sak, SW Thailand. – Sediment. Geol. **239** (3–4): 146–161.
CAHILL, T. & ISACKS, B. L. (1992): Seismicity and shape of the subducted Nazca Plate. – J. Geophys. Res. **97:** 17503–17529.
CAMPOS, J., HATZFELD, D., MADARIAGA, R., LOPEZ, G., KAUSEL, E., ZOLLO, A., IANNACONE, G., FROMM, R., BARRIENTOS, S. & LYON-CAEN, H. (2002): A seismological study of the 1835 seismic gap in south-central Chile. – Phys. Earth Planet. **132:** 177–195.
CIFUENTES, I. L. (1989): The 1960 Chilean Earthquakes. – J. Geophys. Res. **94** (B1): 665–680.
CISTERNAS, M., ATWATER, B. F., TORREJÓN, F., SAWAI, Y., MACHUCA, G., LAGOS, M., EIPERT, A., YOULTON, C., SALGADO, I., KAMATAKI, T., SHISHIKURA, M., RAJENDRAN, C. P., MALIK, J. K., RIZAL, Y. & HUSNI, M. (2005): Predecessors of the giant 1960 Chile earthquake. – Nature **437:** 404–407.
CISTERNAS, M., TORREJAN, F. & GORIGOITIA, N. S. (2012): Amending and complicating Chile's seismic catalog with the Santiago earthquake of 7 August 1580. – J. S. Amer. Earth Sci. **33** (1): 102–109.
CLAGUE, J. J., BOBROWSKY, P. T. & HUTCHINSON, I. (2000): A review of geological records of large tsunamis at Vancouver Island, British Columbia, and implications for hazard. – Quatern. Sci. Rev. **19:** 849–863.
COMTE, D., EISENBERG, A., LORCA, E., PARDO, M., PONCE, L., SARAGONI, R., SINGH, S. K. & SUÁREZ, G. (1986): The 1985 Central Chile earthquake: a repeat of previous great earthquakes in the region? – Science **233:** 449–453.
DARWIN, C. (1846): Geological observations on South America (Part 3: The Geology of the voyage of the Beagle under the command of Captain Fitzroy, R.N.). – London, 279 pp.
DEWEY, J. W. & SPENCE, W. (1979): Seismic Gaps and Source Zones of Recent LargeEarthquakes in Coastal Peru. – Pageoph. **117** (6): 1148–1171.
DUEÑAS-BOHÓRQUEZ, A., DA ROCHA, R. E., KUROYANAGI, A., BIJMA, J. & REICHART, G.-J. (2009): Effect of salinity and seawater calcite saturation state on Mg and Sr incorporation in cultured planktonic foraminifera. – Mar. Micropaleontol. **73:** 178–189.
ENCINAS, A., HERVÉ, F., VILLA-MARTINEZ, R., NIELSEN, S. N., FINGER, K. L. & PETERSON, D. E. (2006): Finding a Holocene marine layer in Algarrobo (33° 22' S), Central Chile. Implications for coastal uplift. – Andean Geol. **33** (2): 339–345.
FUENZALIDA, A., PARDO, M., CISTERNAS, A., DORBATH, L., DORBATH, C., COMTE, D. & KAUSEL, E. (1992): On the geometry of the Nazca Plate subducted under Central Chile (32° S –34.5° S) as inferred from microseismic data. – Tectonophysics **205** (1–3): 1–11.

FUJINO, S., NARUSE, H., MATSUMOTO, D., JARUPONGSAKUL, T., SPHAWAJRUKSAKUL, A. & SAKAKURA, N. (2009): Stratigraphic evidence for pre-2004 tsunamis in southwestern Thailand. – Mar. Geol. **262:** 25–28.

GALLI, P. (2000): New empirical relationships between magnitude and distance for liquefaction. – Tectonophysics **324**: 169–187.

GANNING, B. (1967): Laboratory experiments in the ecological work of rockpool animals with special notes on the ostracod *Heterocypris salinus*. – Helgoländer wiss. Meeresunters. **15:** 27–40.

GARDI, A., LEMOINE, A., MADARIAGA, R. & CAMPOS, J. (2006): Modeling of stress transfer in the Coquimbo region of Central Chile. – J. Geophys. Res. **111** (B4): 1–10.

GELLER, R. J. (2011): Shake-up time for Japanese seismology. – Nature **472:** 407–409.

GERGIS, J. L. & FOWLER, A. M. (2009): A history of ENSO events since A.D. 1525: implications for future climate change. – Climatic Change **92:** 343–387.

GUARNIERI, P., PIRROTTA, C., BARBANO, M. S., DE MARTINI, P. M., PANTOSTI, D., GERARDI, F. & SMEDILE, A. (2009): Paleoseismic Investigation of historical liquefactions along the Ionian coast of Sicily. – J. Earthq. Eng. **13** (1): 68–79, doi: 10.1080/13632460802212030.

HANSON, B. (2005): Learning from Natural Disasters. – Science **308:** 1125.

HAWKES, A. D., SCOTT, D. B., LIPPS, J. H. & COMBELLICK, R. (2005): Evidence for possible precursor events of megathrust earthquakes on the west coast of North America. – Geol. Soc. Amer. Bull. **117:** 996–1008.

HAWKES, A. D., HORTON, B. P., NELSON, A. R., VANE, C. H. & SAWAI, Y. (2011): Coastal subsidence in Oregon, USA, during the giant Cascadia earthquake of AD 1700. – Quatern. Sci. Rev. **30:** 364–376.

HEATON, T. H. & HARTZELL, S. H. (1987): Earthquake hazards on the Cascadia Subduction Zone. – Science **236:** 162–168.

HEKI, K. (2011): A tale of two earthquakes. – Science **332:** 1390–1391.

HERM, D. & PASKOFF, R. (1967): Vorschlag zur Gliederung des marinen Quartärs in Nord- und Mittel-Chile. – N. Jb. Geol. Paläontol. **10:** 577–588.

HORNE, D. J., BRUCE, A. & WHITTAKER, J. E. (2001): Ostracoda. – In: COSTELLO, M. J., EMBLOW, C. S. & WHITE, R. (eds.): European register of marine species: a check-list of the marine species in Europe and a bibliography of guides to their identification. – Coll. Patrimoines Naturels **50:** 244–251.

ISLA, F. I., FLORY, J. Q., MARTÍNEZ, C., FERNÁNDEZ, A. & JAQUE, E. (2012): The evolution of the Bío Bío Delta and the coastal plains of the Arauco Gulf, Bío Bío Region: the Holocene sea-level curve of Chile. – J. Coastal Res. **279:** 102–111.

JANKAEW, K., ATWATER, B. F., SAWAI, Y., CHOOWONG, M., CHAROENTITIRAT, T., MARTIN, M. E. & PRENDERGAST, A. (2008): Medieval forewarning of the 2004 Indian Ocean tsunami in Thailand. – Nature **455:** 1228–1231.

KAGAN, Y. Y. & JACKSON, D. D. (1991): Seismic gap hypothesis: ten years after. – J. Geophys. Res. **96** (B13): 21419–21431.

KELLEHER, J. A. (1972): Rupture zones of large South American earthquakes and some predictions. – J. Geophys. Res. **77:** 2087–2103.

KELSEY, H. M., WITTER, R. C. & HEMPHILL-HALEY, E. (2002): Plate-boundary earthquakes and tsunamis of the past 5500 yr, Sixes River estuary, southern Oregon. – Geol. Soc. Amer. Bull. **114** (3): 298–314.

KELSEY, H. M., NELSON, A. R., HEMPHILL-HALEY, E. & WITTER, R. C. (2005): Tsunami history of an Oregon coastal lake reveals a 4600 yr record of great earthquakes on the Cascadia subduction zone. – Geol. Soc. Amer. Bull. **117** (7–8): 1009–1032.

LE ROUX, J. P., GÓMEZ, C. A., OLIVARES, D. M. & MIDDLETON, H. (2005): Determining the Neogene behavior of the Nazca plate by geohistory analysis. – Geology **33:** 165–168.

LEMOINE, A., MADARIAGA, R. & CAMPOS, J. (2001): Evidence for earthquake interaction in Central Chile: the July 1997 – September 1998 sequence. – Geophys. Res. Lett. **28** (14): 2743–2746.

LEONARD, E. M. & WEHMILLER, J. F. (1992): Low uplift rates and terrace reoccupation inferred from mollusc aminostratigraphy, Coquimbo Bay area, Chile. – Quatern. Res. **38** (2): 246–259.

LOCKRIDGE, P. A. (1985): Tsunamis in Peru-Chile. – World Data Center A for Solid Earth Geophysics, Report SE-**39:** 97 pp., National Geophysical Data Center, Boulder/USA.

LOMNITZ, C. (2004): Major earthquakes of Chile: a historical survey, 1535–1960. – Seismol. Res. Lett. **75** (3): 368–378.

Lorito, S., Romano, F., Atzori, S., Tong, X., Avallone, A., McCloskey, J., Cocco, M., Boschi, E. & Piatanesi, A. (2011): Limited overlap between the seismic gap and coseismic slip of the great 2010 Chile earthquake. – Nature Geosci. **4:** 173–177.

Martin, M. E. & Bourgeois, J. (2012): Vented sediments and tsunami deposits in thePuget Lowland, Washington – differentiating sedimentary processes. – Sedimentology **59** (2): 419–444.

Martínez, C., Quezada, M. & Rubio, P. (2011): Historical changes in the shoreline and littoral processes on a headland bay beach in central Chile. – Geomorphology **135:** 80–96.

May, S. M., Vött, A., Brückner, H., Grapmayer, R., Handl, M. & Wennrich, V. (2012): The Lefkada barrier and beachrock system (NW Greece) – controls on coastal evolution and the significance of extreme wave events. – Geomorphology **139-140:** 330–347.

Meisch, C. (2000): Freshwater Ostracoda of Western and Central Europe. – Süßwasserfauna von Mitteleuropa **8/3:** 522 pp., Spektrum, Heidelberg/Berlin.

Melnick, D., Bookhagen, B., Echtler, H. P. & Strecker, M. R. (2006): Coastal deformation and great subduction earthquakes, Isla Santa Maria, Chile (37° S). – Geol. Soc. Amer. Bull. **118** (11–12): 1463–1480.

Melnick, D., Cisternas, M., Moreno, M. & Norambuena, R. (2012): Estimating coseismic coastal uplift with an intertidal mussel: calibration for the 2010 Maule Chile earthquake (Mw = 8.8). – Quatern. Sci. Rev. **42:** 29–42.

Métois, M., Socquet, A. & Vigny, C. (2012): Interseismic coupling, segmentation and mechanical behavior of the Central Chile subduction zone. – J. Geophys. Res. **117** (B3): B03406, doi: 10.1029/2011JB008736.

Moreno, M. S., Klotz, J., Melnick, D., Echtler, H. & Bataille, K. (2008): Active faulting and heterogeneous deformation across a megathrust segment boundary from GPS data, south central Chile (36–39° S). – Geochem. Geophys. Geosyst. **9:** Q12024, doi: 10.1029/2008GC002198.

Moreno, M. S., Bolte, J., Klotz, J. & Melnick, D. (2009): Impact of megathrust geometry on inversion of coseismic slip from geodetic data: Application to the 1960 Chile earthquake. – Geophys. Res. Lett. **36** (16): L16310.

Moreno, M. S., Rosenau, M. & Oncken, O. (2010): 2010 Maule earthquake slip correlates with pre-seismic locking of Andean subduction zone. – Nature **467:** 198–202.

Moreno, M. S., Melnick, D., Rosenau, M., Bolte, J., Klotz, J., Echtler, H., Baez, J., Bataille, K., Chen, J., Bevis, M., Hase, H. & Oncken, O. (2011): Heterogeneous plate locking in the South-Central Chile subduction zone: Building up the next great earthquake. – Earth Planet. Sc. Lett. **305** (3–4): 413–424.

Nelson, A. R. & Manley, W. F. (1992): Holocene coseismic and aseismic uplift of Isla Mocha, south-Central Chile. – Quatern. Int. **15–16:** 61–76.

Nishenko, S. P. (1985): Seismic potential for large and great interplate earthquakes along the Chilean and Southern Peruvian margins of South America: A quantitative reappraisal. – J. Geophys. Res. **90** (B5): 3589–3615.

Nuñez, L., Varela, J., Casamiquela, R. & Villagrán, C. (1994): Reconstruccion multidisciplinaria de la ocupacion prehistorica de Quereo, Centro de Chile. – Lat. Amer. Antiq. **5** (2): 99–118.

Ortega, C., Vargas, G., Rutllant, J. A., Jackson, D. & Méndez, C. (2012): Major hydrological regime change along the semiarid western coast of South America during the early Holocene. – Quatern. Res. **78:** 513–527.

Ota, Y. & Paskoff, R. (1993): Holocene deposits on the coast of north-Central Chile: radiocarbon ages and implications for coastal changes – Rev. Geol. Chile **20** (1): 25–32.

Otvos, E. G. (2000): Beach ridges – definitions and significance. – Geomorphology **32:** 83–108.

Ozawa, S., Nishimura, T., Suito, H., Kobayashi, T., Tobita, M. & Imakiire, T. (2011): Coseismic and postseismic slip of the 2011 magnitude-9 Tohoku-Oki earthquake. – Nature **475:** 373–376.

Pardo, M., Comte, D., Monfret, T., Boroschek, R. & Astroza, M. (2002a): The October 15, 1997 Punitaqui earthquake (Mw = 7.1): a destructive event within the subducting Nazca plate in Central Chile. – Tectonophysics **345** (1–4): 199–210.

Pardo, M., Comte, D. & Monfret, T. (2002b): Seismotectonic and stress distribution in the Central Chile subduction zone. – J. S. Amer. Earth Sci. **15** (1): 11–22.

Paskoff, R. P. (1970): Recherches géomorphologiques dans le Chili semi-aride. – 420 pp., Biscaye, Bordeaux.

Paskoff, R. P. (1973): Radiocarbon dating of marine shells taken from the north and central coast of Chile. –Proceedings of the IX International INQUA Congress, Abstract: 281–282; Christchurch, New Zealand.

PFEIFFER, M., LE ROUX, J. P., SOLLEIRO-REBOLLEDO, E., KEMNITZ, H., SEDOV, S. & SEGUEL, O. (2011): Preservation of beach ridges due to pedogenic calcrete development in the Tongoy palaeobay, North-Central Chile. – Geomorphology **132** (3–4): 234–248.

PLAFKER, G. & SAVAGE, J. C. (1970): Mechanism of the Chilean Earthquakes of May 21 and 22, 1960. – Geol. Soc. Amer. Bull. **81** (4): 1001–1030.

QUEZADA, J., GONZALEZ, G., DUNAI, T., JENSEN, A. & JUEZ-LARRE, J. (2007): Pleistocene littoral uplift of northern Chile: ^{21}Ne age of the upper marine terrace of Caldera-Bahia Inglesa area. – Rev. Geol. Chile **34:** 81–96.

RADTKE, U. (1987): Marine terraces in Chile (22° – 32° S). – Geomorphology, chronostratigraphy, and neotectonics. – In: RABASSA, J. (ed.): Quatern. S. Amer. and Antarct. Peninsula **5:** 239–256, Balkema, Rotterdam.

RADTKE, U. (1989): Marine Terrassen und Korallenriffe. – Das Problem der quartären Meeresspiegelschwankungen erläutert an Fallstudien aus Chile, Argentinien und Barbados. – Düsseld. Geograph. Schrift. **27:** 246 S.

RANERO, C. R., VON HUENE, R., WEINREBE, W. & REICHERT, C. (2006): Tectonic processes along the Chile convergent margin. – In: ONCKEN, O., CHONG, G., FRANZ, G., GIESE, P., GÖTZE, H.-J., RAMOS, V., STRECKER, M. & WIGGER, P. (eds): The Andes – Active Subduction Orogeny, 91–121, Springer.

REIMER, P. J., BAILLIE, M. G. L., BARD, E., BAYLISS, A., BECK, J. W., BLACKWELL, P. G., RAMSEY, C. B., BUCK, C. E., BURR, G. S., EDWARDS, R. L., FRIEDRICH, M., GROOTES, P. M., GUILDERSON, T. P., HAJDAS, I., HEATON, T. J., HOGG, A. G., HUGHEN, K. A., KAISER, K. F., KROMER, B., MCCORMAC, F. G., MANNING, S. W., REIMER, R. W., RICHARDS, D. A., SOUTHON, J. R., TALAMO, S., TURNEY, C. S. M., VAN DER PLICHT, J. & WEYHENMEYER, C. E. (2009): IntCal09 and Marine09 Radiocarbon Age Calibration Curves, 0–50,000 Years cal BP. – Radiocarbon **51** (4): 1111–1150.

REINHARDT, E. G., NAIRN, R. B. & LOPEZ, G. (2010): Recovery estimates for the Río Cruces after the May 1960 Chilean earthquake. – Mar. Geol. **269** (1–2): 18–33.

RODRIGUEZ, M. P., CARRETIER, S., CHARRIER, R., SAILLARD, M., REGARD, V., HÉRAIL, G., HALL, S., FARBER, D. & AUDIN, L. (2013): Geochronology of pediments and marine terraces in north-central Chile and their implications for Quaternary uplift in the Western Andes. – Geomorphology **180–181:** 33–46.

SAILLARD, M., HALL, S. R., AUDIN, L., FARBER, D. L., HÉRAIL, G., MARTINOD, J., REGARD, V., FINKEL, R. C. & BONDOUX, F. (2009): Non-steady long-term uplift rates and Pleistocene marine terrace development along the Andean margin of Chile (31° S) inferred from ^{10}Be dating. – Earth Planet. Sci. Lett. **277** (1–2): 50–63.

SAILLARD, M., RIOTTE, J., REGARD, V., VIOLETTE, A., HÉRAIL, G., AUDIN, L. & RIQUELME, R. (2012): Beach ridges U-Th dating in Tongoy bay and tectonic implications for a peninsula-bay system, Chile. – J. S. Amer. Earth Sci. **40:** 77–84.

SANDWEISS, D. H. (1986): The Beach Ridges at Santa, Peru: El Niño, Uplift, and Prehistory. – Geoarchaeology **1** (1): 17–28.

SATAKE, K. & ATWATER, B. F. (2007): Long-term perspectives on giant earthquakes and tsunamis at subduction zones. – Annu. Rev. Earth Planet. Sci. **35** (1): 349–374.

SAWAI, Y. (2001): Episodic emergence in the past 3000 years at the Akkeshi Estuary, Hokkaido, Northern Japan. – Quatern. Res. **56** (2): 231–241.

SAWAI, Y., SATAKE, K., KAMATAKI, T., NASU, H., SHISHIKURA, M., ATWATER, B. F., HORTON, B. P., KELSEY, H. M., NAGUMO, T. & YAMAGUCHI, M. (2004): Transient uplift after a 17th century earthquake along the Kuril Subduction Zone. – Science **306:** 1918–1920.

STEIN, S. (2006): Limitations of a young science. – Seismol. Res. Lett. **77** (3): 351–353.

STEIN, S. (2008): The seismogenic zone of subduction thrust faults. – Seismol. Res. Lett. **79** (4): 572–573.

STOPA, J. E., CHEUNG, K. F., TOLMAN, H. L. & CHAWLA, A. (2012): Patterns and cycles in the Climate Forecast System Reanalysis wind and wave data. – Ocean Modelling, in press, http://dx.doi.org/10.1016/j.ocemod.2012.10.005.

VARGAS, G., FARIAS, M., CARRETIER, S., TASSARA, A., BAIZE, S. & MELNICK, D. (2011): Coastal uplift and tsunami effects associated to the 2010 Mw8.8 Maule earthquake in Central Chile. – Andean Geol. **38** (1): 219–238.

VICUÑA-MACKENNA, B. (1877): Ensayo histórico sobre el clima de Chile. – Imprenta El Mercurio, Valparaiso.

VIGNY, C., RUDLOFF, A., RUEGG, J.-C., MADARIAGA, R., CAMPOS, J. & ALVAREZ, M. (2009): Upper plate deformation measured by GPS in the Coquimbo Gap, Chile. – Phys. Earth Planet. Int. **175** (1–2): 86–95.

VILLAGRÁN, C. & VARELA, J. (1990): Palynological evidence for increased aridity on the Central Chilean coast during the Holocene. – Quatern. Res. **34** (2): 198–207.

VÖTT, A. (2007): Relative sea level changes and regional tectonic evolution of seven coastal areas in NW Greece since the mid-Holocene. – Quatern. Sci. Rev. **26:** 894–919.

WELLS, A. & GOFF, J. (2006): Coastal dune ridge systems as chronological markers of palaeoseismic activity: a 650-yr record from southwest New Zealand. – The Holocene **16:** 543–550.

WILLIAMS, A. N. (2012): The use of summed radiocarbon probability distributions in archaeology: a review of methods. – J. Archaeol. Sci. **39:** 578–589.

YEATS, R. S., SIEH, K. & ALLEN, C. R. (1997): The Geology of Earthquakes. – Oxford Univ. Press, 568 pp., New York.

YOUD, T. L. (1977): Discussion of 'Brief review of liquefaction during earthquakes in Japan'. – In: KURIBAYASHI, E. & TATSUOKA, F. (1975): Soil and Foundations **17** (1): 82–85.

Addresses of the authors:

Dr. Simon Matthias May (corresponding author), Anna Pint, Gilles Rixhon, Dieter Kelletat and Helmut Brückner, Institute of Geography, University of Cologne, Albertus-Magnus-Platz, 50923 Köln (Cologne), Germany, e-mail: mays@uni-koeln.de, Phone:+49 221 470 4841, Fax:+49 221 470 5124.

Volker Wennrich, Institute for Geology and Mineralogy, University of Cologne, Zülpicher Str. 49 a, 50674 Cologne, Germany.